MATHEMATICAL MODELLING OF A BINARY SYSTEM OF COPPER AND LEAD BIOSORPTION IN A FIXED BED COLUMN

FELICIA OMOLARA AFOLABI[1] & PAUL MUSONGE[2]
[1]Department of Chemical Engineering, Durban University of Technology, South Africa
[2]Institute of Systems Science, Durban University of Technology, South Africa

ABSTRACT

Since it is extremely uncommon for wastewater to have a single metal ion, it is crucial to investigate the impact of metal ion coexistence when applying the biosorption method for industrial-scale wastewater treatment. In the industrial treatment application and scale-up of biosorption processes, numerous operating parameters are crucial. However, the initial concentration is a major operating parameter influencing adsorption of heavy metals. In this study, the effect of initial metal ion concentrations on the adsorption of Cu^{2+} and Pb^{2+} in a binary solute system was investigated in a column study using natural orange peels as an adsorbent. The experimental data was fitted to the current dynamic models (Thomas, Yoon–Nelson and Bohart–Adams). Since the binding site was rapidly saturated, a rise in the influent concentration produced a steeper breakthrough curve that was closer to the origin. For both metals, the breakthrough time dropped with increased initial concentration. For all three of the starting concentrations that were examined (10, 50, and 100 mg/L), the adsorption capacity of Pb^{2+} was consistently greater than that of Cu^{2+}, and this difference was dependent upon the binding strength of Pb^{2+}. The experimental results showed good performance from the Yoon–Nelson and Thomas models, with a strong correlation coefficient ($R^2 > 0.9$). The results obtained have shown that the performance of the fixed bed column conducted at a laboratory scale was efficient throughout the experimentation hence, this can be scaled up for industrial treatment applications.

Keywords: biosorption, heavy metal, bi-solute, wastewater, modelling.

1 INTRODUCTION

Pollution of water bodies has become a major concern in many countries worldwide because water is life. Water is an indispensable resource for plant, animal and human beings. Availability of clean and potable water is also affected by the yearly dwindling rainfall pattern which in turn impact the environment. South Africa's annual rainfall average is less than the global average and is not dispersed equally throughout the nation's regions [1]. Furthermore, technological advancement is another menace influencing the supply of pure water. In addition, many industrial activities generate wastewater containing pollutants that are hazardous to plant, animal, and human health. Industries such as mining, electroplating, smelting, explosive manufacturing and batteries generate wastewater containing heavy metals which affect surface and underground water [2]. Some of the heavy metals found in industrial wastewater include copper, lead, iron, manganese, nickel, cadmium, zinc [3]. These heavy metals are non-biodegradable and accumulate in the soil and food chain. The presence of these heavy metals in water has adverse effects on human health either through inhalation or absorption. Hence, it is necessary to treat wastewater generated from industrial activities before it is discharged into the water bodies.

Copper and lead are toxic metals mostly found in industrial wastewater. These heavy metals are toxic and have harmful effects on human health such as brain damage, liver and kidney disease, mental retardation, gastrointestinal damage, neurotoxicity, dizziness, diarrhoea and cancer [4]. Tertiary treatment techniques can be used to remediate wastewater containing non-biodegradable pollutants, which pose a major hazard to the environment.

WIT Transactions on Ecology and the Environment, Vol 262, © 2024 WIT Press
www.witpress.com, ISSN 1743-3541 (on-line)
doi:10.2495/SDP240451

Some of the techniques suitable for wastewater treatment include chemical precipitation, electrochemical, coagulation/flocculation, membrane separation, solvent extraction, adsorption, ion exchange and reverse osmosis [5]. Except for the adsorption technique, other treatment methods are costly and generate large volumes of sludge which also increase the operating cost [6]. Substances can be extracted from the liquid phase using a surface technique called adsorption. Heavy metals have been effectively removed from wastewater using this technology [7]. The adsorption technique has advantages such as ease of operation, less expensive, efficient, applicable at low concentration and low sludge generation [8].

Recently, researchers have focused on the use of biological materials for the adsorption of contaminants from wastewater also referred to as the biosorption process. Agricultural wastes are abundantly available in nature and efficient for the adsorption of heavy metals. Different agricultural wastes have been utilised for adsorption studies of heavy metals which have proven effective and efficient [9]. Such biosorbents include, rice husk, banana peels, orange peels, eggshell, bagasse, watermelon rind, apple pomace [10]–[16]. The highly porous surface of biosorbents and the presence of metal-binding functional groups on their surface facilitate the adsorption of metal ions within the pores [17].

In this study, Pb^{2+} and Cu^{2+} were removed from wastewater using orange peels as a biosorbent. The most common citrus fruit in South Africa is orange, which grows on over 45,000 hectares of cultivated land to produce 60% of all citrus fruits. An estimated 1.5 million mega tons of oranges are produced in South Africa each year, some of which are exported or used to make fruit juice [18]. Orange peels that are unwanted constitute a substantial quantity of waste from homes, businesses, and markets that are dumped in landfills. These wastes can be utilised as inexpensive, easily accessible, and environmentally beneficial adsorbents to remove Cu^{2+} and Pb^{2+} from wastewater, therefore minimising pollution levels in the environment. To achieve the aim of this study, a fixed-bed column was used for the adsorption process. Many studies reported on adsorption are focused on batch mode operation which does not represent the typical industrial treatment wastewater plant. It is expedient to take research work beyond laboratory level to benefit the society and enhance community engagement. Therefore, the use of a fixed-bed column will allow for scale-up of the laboratory experiments for industrial applications.

In addition, the adsorption study of bi-solute system of Cu^{2+} and Pb^{2+} from wastewater in a dynamic mode is a unique aspect of this study. Although, the composition of wastewater depends on its source nevertheless, wastewater rarely contains a single solute. Hence, the adsorption behaviour of heavy metal ions and efficiency of adsorbents in the presence of other metal ions is a new area of research to explore. Numerous studies on the adsorption of metal ions using fixed-bed columns have been published; however, no investigations on the bi-solute system of Pb^{2+} and Cu^{2+} using orange peels have been published. There are many operating parameters involved in adsorption process however, this study is focused on initial concentration which is a major factor. While the optimum conditions obtained from the single solute system are used in this study. The operating parameters responsible for adsorption in column studies, such as bed height and flowrate, were investigated in a single solute system utilising orange peels. In addition, the experimental data was fitted with existing dynamic models such as the Thomas model, Yoon–Nelson and Bohart–Adams models to determine the breakthrough curve parameters.

2 MATERIALS AND METHODS

2.1 Preparation of metal solution

$Cu(N0_3)_2.3H_20$ and $Pb(N0_3)_2$ in the appropriate concentrations were dissolved in distilled water to create a metal solution with a combination of copper and lead ions. The stock solution was further diluted to obtain the required initial concentration of the metal solution. The pH of the solutions was adjusted to 5.5 using 0.1 M H_2S0_4 or 0.1 M NaOH, respectively. All the chemicals used were of analytical grade purchased from Sigma Aldrich Chemical Company.

2.2 Preparation of the biosorbent

Orange peels were sourced from a neighbourhood market in Durban, KwaZulu Natal province in South Africa. Sand and filth were eliminated from the garbage by washing it with distilled water after collection. The biosorbent was prepared following the method discussed in our previous work [19]. The prepared biosorbent was sieved to obtain a particle size in the range 800–1000 µm used in the column studies. The biosorbent's surface functional groups were examined using Fourier Transform Infrared Spectroscopy (FT-IR) (Perkin Elmer, Frontier, Waltham, MA, USA) both before and following adsorption. Using a scanning electron microscope (SEM) (FEI Nova NanoSEM 230, Lausanne, Switzerland) and energy dispersive x-ray spectroscopy (EDS) (Oxford X-Max detector, Oxford, UK and INCA software v7.3, Stuttgart, Germany) analysis, the morphological structure and elemental composition of the biosorbent were determined.

2.3 Continuous biosorption study

The glass column utilised was a portable laboratory scale, measuring 50 mm in height and 2.5 mm inner diameter. The column was designed in such a way that the height could be adjusted and operated in a downward flow. A layer of cotton wool was placed at the top and bottom of the biosorbent in the column to keep the biosorbent in position and prevent channelling. A peristaltic pump (Flexflo A1N11E-4T) was used for feeding the inlet solution into the column at a constant flowrate and bed height of 3 mL/min and 3 cm respectively. A binary solution of Cu^{2+} and Pb^{2+} at the initial concentration of 10 mg/L, 50 mg/L and 100 mg/L were used to evaluate the performance of the biosorbent. Samples were collected at the outlet and analysed to determine the concentrations of Cu^{2+} and Pb^{2+} ions in the solution. Samples were taken periodically until the outflow concentration was equal to the inlet concentration. Syringe filters (0.45 µm) and Whatman filter paper (150 mm) were used to filter the samples. The micro-plasma atomic emission spectrophotometer (MP–AES, MY 18379001, Agilent, USA) was used to analyse the concentration of Cu^{2+} and Pb^{2+} ions remaining in the solution after adsorption. All the experiments were carried out at a room temperature of 25°C ± 2°C. The metal uptake, q (mg/g) is expressed in eqn (1):

$$q = \frac{C_0 Q}{1000m} \int_0^t \left(1 - \frac{C_t}{C_0}\right) dt \tag{1}$$

where Q is the volumetric flow rate (mL/min^{-1}), C_t is the concentration at time t (mg/L), m is the mass of the adsorbent (g), and C_o is the adsorbed concentration (mg/L).

2.4 Breakthrough: Mathematical model

In this study, three dynamic models were applied to the experimental data namely, Thomas, Yoon–Nelson and Bohart–Adams.

2.4.1 Thomas model

Thomas model is the most popular model for predicting the breakthrough curve and estimating the adsorptive capacity of adsorbents. According to this model, a plug flow without any axial dispersion and pseudo-second-order adsorption kinetics are associated with an equilibrium Langmuir isotherm [20], [21]. The expression of the model is stated in eqn (2):

$$\frac{C_t}{C_o} = \frac{1}{1+ exp\left(\frac{K_{TH}}{Q}\left(q_o m - C_o V_{eff}\right)\right)} \tag{2}$$

The linearised form of the equation is stated below:

$$\ln\left[\left(\frac{C_o}{C_t}\right) - 1\right] = \left(\frac{K_{TH} q_o m}{Q}\right) - \left(\frac{K_{TH} C_o V_{eff}}{Q}\right) \tag{3}$$

The variables in this equation are: Q is the flow rate (mL/min), m is the mass of the loaded adsorbent (g), V_{eff} is the effluent volume (mL), C_0 is the influent concentration (mg/L), and C_t is the effluent concentration at time t (mg/L). Additionally, K_{TH} is the Thomas constant (mL/mg-min).

2.4.2 Yoon–Nelson model

Yoon–Nelson developed a model which predicted the adsorption of gases in activated coal. This model proposes that the likelihood of adsorbate sorption and the probability of sorbate breakthrough on the sorbent without axial dispersion are directly related to the rate at which the probability of adsorbate molecule adsorption decreases [22]. The model equation is expressed below:

$$\frac{C_o}{C_t} = \frac{1}{1+ e^{K_{YN}(\tau - t)}} \tag{4}$$

Eqn (5) below expresses the equation in its linear form:

$$\ln\left(\frac{C_t}{C_o - C_t}\right) = K_{YN} t - \tau K_{YN} \tag{5}$$

where K_{YN} is the Yoon–Nelson rate constant (min^{-1}) and τ is the time at which effluent concentration reaches 50% of the inlet concentration.

2.4.3 Bohart–Adams model

Assuming irreversible adsorption, this model analyses the dynamic behaviour of the column by showing that the amount of a solute adsorbed is precisely proportional to its concentration in the bulk solution and the amount of adsorbent that is still adsorptive. It also presupposes perfect plug flow devoid of axial dispersion [23]. The model equation is stated below:

$$\frac{C_t}{C_o} = \frac{e^{K_{AB} C_o t}}{e^{(K_{AB} N_o Z / U_o) - 1 + e^{K_{AB} C_o t}}} \tag{6}$$

The model equation linearised form is provided as:

$$\ln\left(\frac{C_t}{C_o}\right) = K_{AB}\, C_o t - K_{AB} N_o \left(\frac{Z}{U_o}\right) \tag{7}$$

where N_o is the maximum volumetric sorption capacity in mg/L, Z is the bed height in cm, U_o is the superficial velocity in cm/min, and K_{AB} is the kinetic constant in L/mg-min.

3 RESULTS AND DISCUSSIONS

3.1 Analytical results of biosorbent

3.1.1 FTIR spectroscopy analysis

FTIR spectroscopy analysis is one of the analytical techniques used to characterise biosorbents. FTIR analysis is used to determine the functional groups resident on the surface of biosorbents before and after adsorption studies. This analysis helps to explain the tendency of a particular adsorbent to efficiently adsorb heavy metals before adsorption and the nature of the interaction between the functional groups and the metal ions in the solution thereby revealing the adsorption mechanism. The result as shown in Fig. 1, represent the plot of the transmittance (%) against the wavenumber (cm^{-1}) ranging from 4,000 to 500 cm^{-1}. The native orange peels (natural-OP) spectrum revealed a significant peak at 3,382.6 cm^{-1}, indicating an O-H group with intermolecular bond comprising of phenols and alcohols. Like alkanes found in pulp, the peaks at 2,918.92 cm^{-1} and 2,850.97 cm^{-1} represent the availability of a saturated C-H substitution bond on the surface of the orange peels. Aldehydes and ketones are responsible for the presence of carbonyl group C=O bond and the unsaturated alkene group C=C bond, which are visible at 1,734.38 cm^{-1} and 1,607.04 cm^{-1} respectively. The peaks are 1,374.74 cm^{-1} and 887.26 cm^{-1} suggest the presence of carboxyl functional group C-O-H which can be attributed to citric acid found in orange peels. Orange peels tendency to adsorb cations is revealed by the abundance of hydroxyl and carboxyl groups present on the surface of the biosorbent. The presence of these groups enhances the biosorption of metal ions during adsorption process.

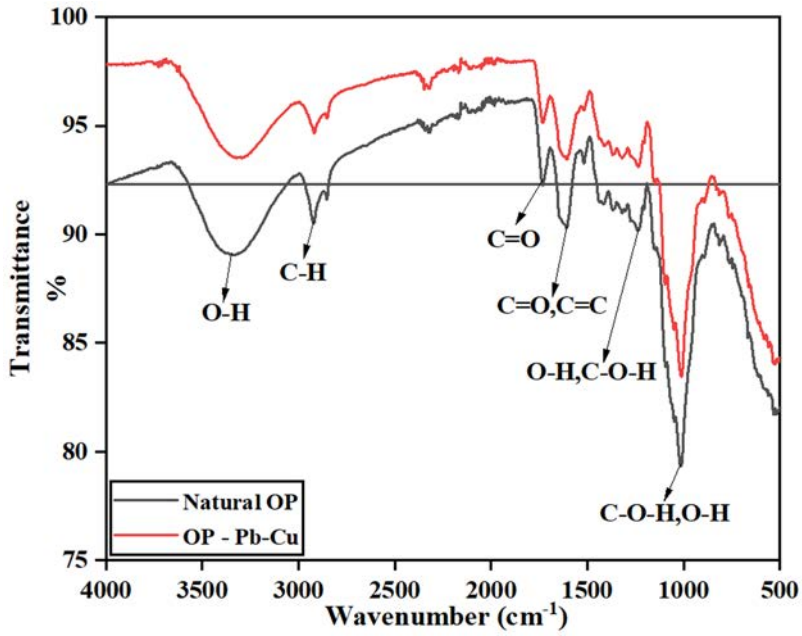

Figure 1: FTIR analysis of natural orange peels (OP) and OP loaded with Pb^{2+} and Cu^{2+}.

After adsorption, the spectrum of orange peels loaded with lead and copper ions showed some significant shifts in the peaks specified for the natural orange peels. The interaction between the Cu^{2+} and Pb^{2+} in the solution and the functional groups on the biosorbent surface is responsible for these alterations. Following adsorption, there was a notable shift in the peaks that represented the O-H and C-O-H stretching, which are significant to the adsorption of lead and copper. This indicates that the adsorption of lead and copper was significantly influenced by hydroxyl and carboxyl groups.

3.1.2 SEM–EDS analysis

The SEM analysis is an analytical technique which reveals the surface structure of an adsorbent while the EDS shows the chemical composition of the adsorbent. Fig. 2(a) and (b) represents the surface structure of orange peels biosorbent before and after adsorption of Pb^{2+} and Cu^{2+} respectively. The surface of natural OP before adsorption exhibits a rough, irregular and heterogenous surface. These features showed that orange peels have the potential to adsorb Pb^{2+} and Cu^{2+} since the heterogenous surface indicate different active sites on the surface of the biosorbent. After the adsorption of Pb^{2+} and Cu^{2+}, the surface of the biosorbent became whitish and shiny which can be attributed to the physiochemical interactions between the metal ions in the aqueous solution and the functional groups present on the surface of the biosorbent. In addition, the surface had a rough structure with small irregular particle deposits dispersed over it.

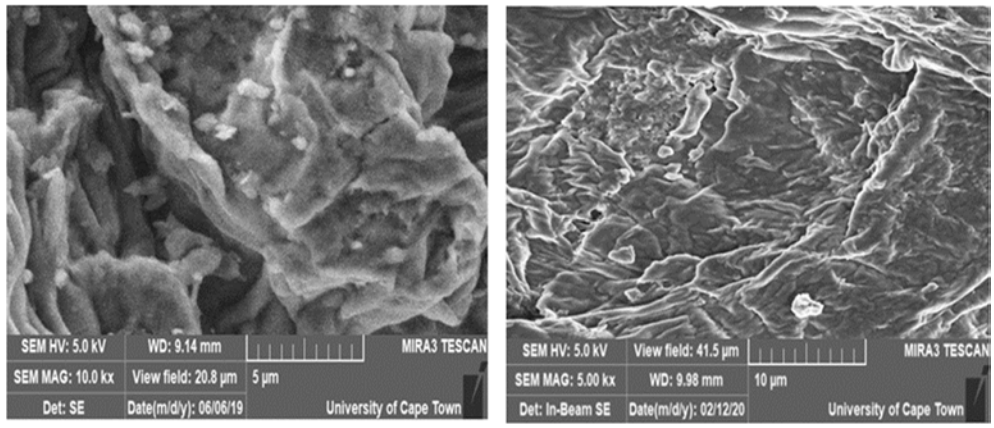

(a) (b)

Figure 2: SEM analysis of orange peels. (a) Before; and (b) After adsorption of Pb^{2+} and Cu^{2+}.

Table 1 shows the EDS results of orange peels biosorbent prior to and after adsorption studies. The chemical composition of orange peels before adsorption indicated that carbon, oxygen, magnesium, sulphur, potassium, and calcium were present in the biosorbent. However, after biosorption, the composition revealed the presence of carbon, oxygen, lead and copper. It is evident that other elements vanished except for carbon and hydrogen while Pb^{2+} and Cu^{2+} replaced the elements. Therefore, the EDS analysis ascertained that Pb^{2+} and Cu^{2+} were favourably adsorbed on the surface of the biosorbent due to the physiochemical interactions between the elements on the surface of the biosorbent and the metal ions in the solution thus suggesting ion-exchange mechanism. This result supports the SEM analysis.

Table 1: Elemental composition of orange peels prior to and after adsorption of Pb^{2+} and Cu^{2+}.

Elemental composition (%)	C	O	Mg	S	K	Ca	Cu	Pb
Natural OP	56.79	41.21	0.28	0.17	0.37	1.18	–	–
OP-Pb-Cu	42.78	50.40	–	–	–	–	2.13	4.69

3.2 Influence of initial concentration on the binary solute system of Pb^{2+} and Cu^{2+}

The impact of initial concentration on the binary solute system of Cu^{2+} and Pb^{2+} was investigated, considering the initial concentrations (10 mg/L, 50 mg/L, and 100 mg/L) of Cu^{2+} and Pb^{2+} at a ratio of 1:1 with a constant bed height of 3 cm and a flow rate of 3 mL/min. The comparison of the breakthrough curves representing the binary systems of Cu^{2+} and Pb^{2+} is depicted in Figs 3–5. The breakthrough curves are represented by the normal concentration (ratio of effluent metal ion concentration to the influent metal ion concentration) against the time profile which depicts the typical S-shapes. The binary breakthrough curves for Pb^{2+} and Cu^{2+} demonstrated that each metal ion has a different biosorption capability, and the curves indicate that Pb^{2+} has a stronger affinity for orange peels. For every initial concentration selected, the biosorption capacity of Pb^{2+} was consistently greater than the biosorption capacity of Cu^{2+}. This demonstrates that Pb^{2+} has a greater affinity for orange peels regardless of the initial concentration of metal ions. This was also reported for the batch experiments and the individual metal ions.

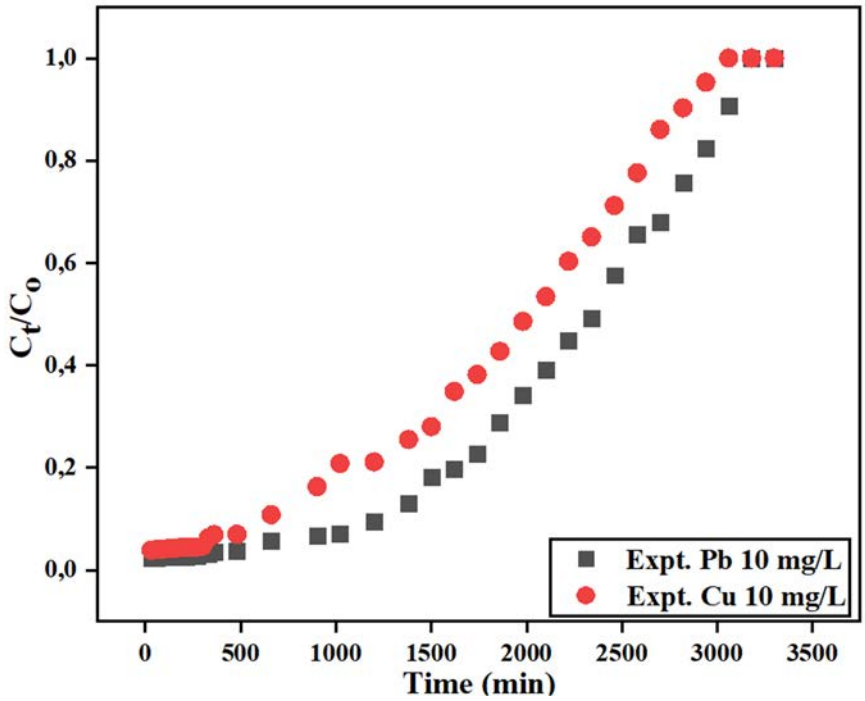

Figure 3: Experimental breakthrough curves of Cu^{2+} and Pb^{2+} in binary solution using orange peels.

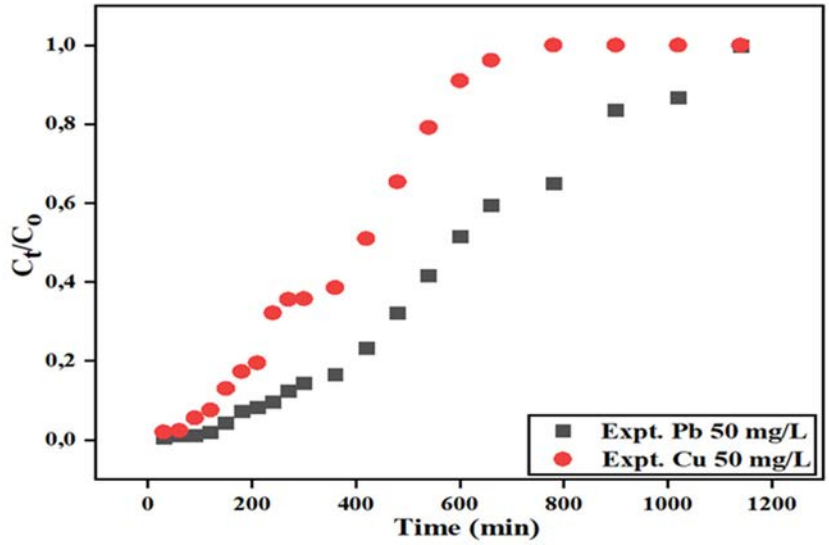

Figure 4: Experimental breakthrough curves of Cu^{2+} and Pb^{2+} in binary solution using orange peels.

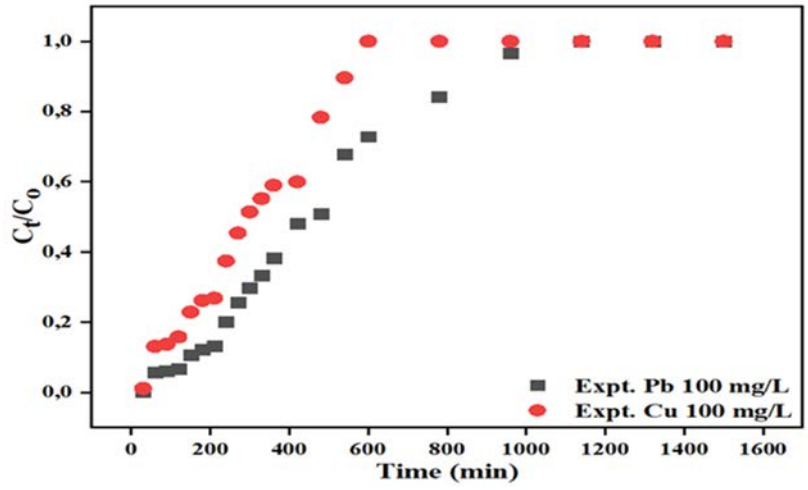

Figure 5: Experimental breakthrough curves of Cu^{2+} and Pb^{2+} in binary solution using orange peels.

Considering Figs 3–5, the breakthrough time dropped as the initial concentration of both metal ions increased. Since the binding sites were rapidly saturated, a rise in the starting metal ion concentration produced a sharp rise in the breakthrough curve that moved the curve nearer to the origin. Additionally, complete breakthrough curves for the various initial concentrations used were achieved for both metal ions. Copper biosorption breakthrough curves reached a breakthrough point more quickly than Pb^{2+}. Moreover, factors like covalent

binding, and the hydrated ionic radius that describe the binding strength of the metal ions can be used to explain the behaviour of Cu^{2+} and Pb^{2+} in a binary system. The electrostatic binding of metal ions is correlated with an alteration in the hydration angle of the water molecules. A change in state may occur and the metal ion may gather at the biosorbent interface if the metal ion is not able to firmly hold onto the hydrated water molecules [24]. Larger ions that are less highly hydrated tend to collect near the interface when comparing the crystal radii of ions with the same charge, such as Pb^{2+} and Cu^{2+}. Pb^{2+} has a hydration ion radius of 4.01 which is smaller than Cu^{2+} having 4.19, due to its higher propensity for adsorption on biosorbent. Less highly hydrated ions tend to gather at the interface. Furthermore, the inclination and capacity of the metal ion to establish covalent bonds with the functional groups on the surface of the biosorbent increases with a higher covalent binding index. Larger ions can therefore fit into a binding site and bind to multiple groups on an adsorbent surface at once. The covalent binding strength of Pb^{2+} is 7.18 while that of Cu^{2+} is 6.41, this explains why Pb^{2+} has stronger affinity for orange peels. Therefore, it can be said that increased covalent binding and an ionic radius with a lower hydrated radius are the causes of Pb^{2+} tending towards greater binding and affinity.

3.3 Application of breakthrough curve models to the binary system of Cu^{2+} and Pb^{2+}

The current models, Thomas, Yoon–Nelson, and Bohart–Adams, were used to fit the breakthrough curves that were obtained from the binary systems of Cu^{2+} and Pb^{2+} for the various influent concentrations that were evaluated. The graphs illustrating the model fittings are depicted in Figs 6–8, and Table 2 summarises the values obtained for the model parameters.

3.3.1 Thomas model

The Thomas model demonstrated in Fig. 6 that a rise in starting concentration led to a reduction in K_{Th} values and an increase in q_o values in proportion. For both Pb^{2+} and Cu^{2+},

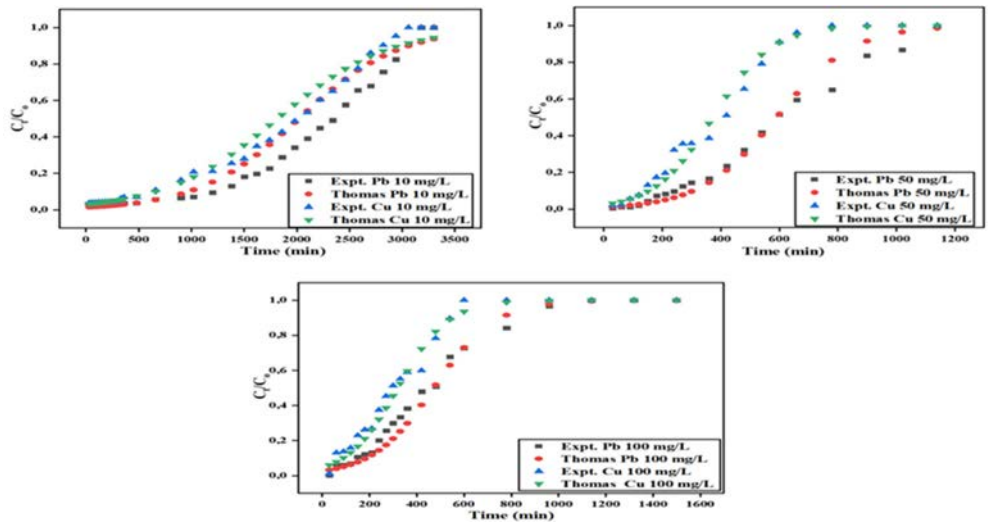

Figure 6: Breakthrough curves of Pb^{2+} and Cu^{2+} at initial concentration of 10, 50 and 100 mg/L fitted into Thomas model.

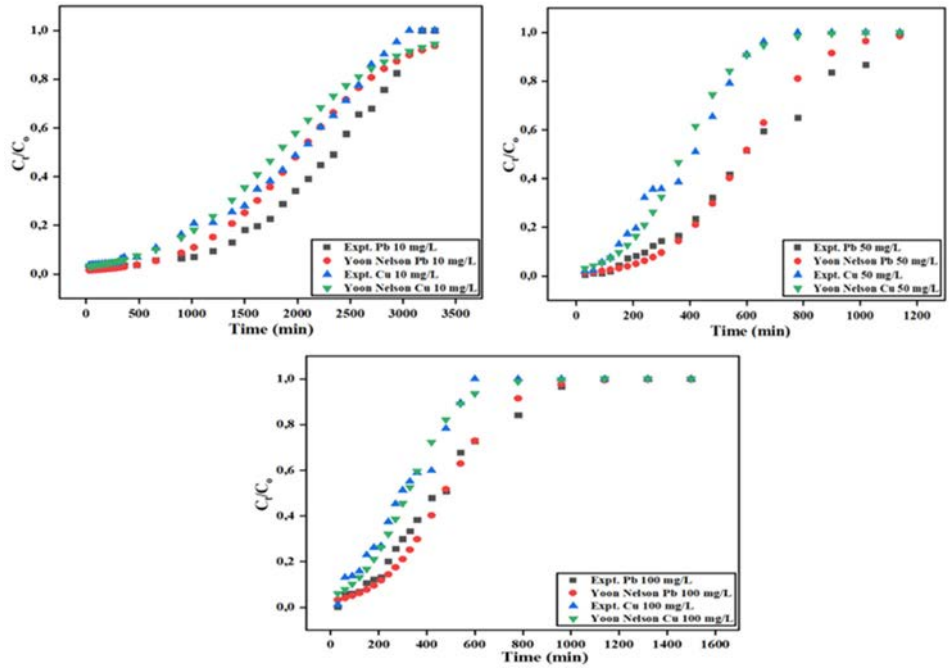

Figure 7: Breakthrough curves of Pb^{2+} and Cu^{2+} at initial concentration of 10, 50 and 100 mg/L fitted into Yoon–Nelson model.

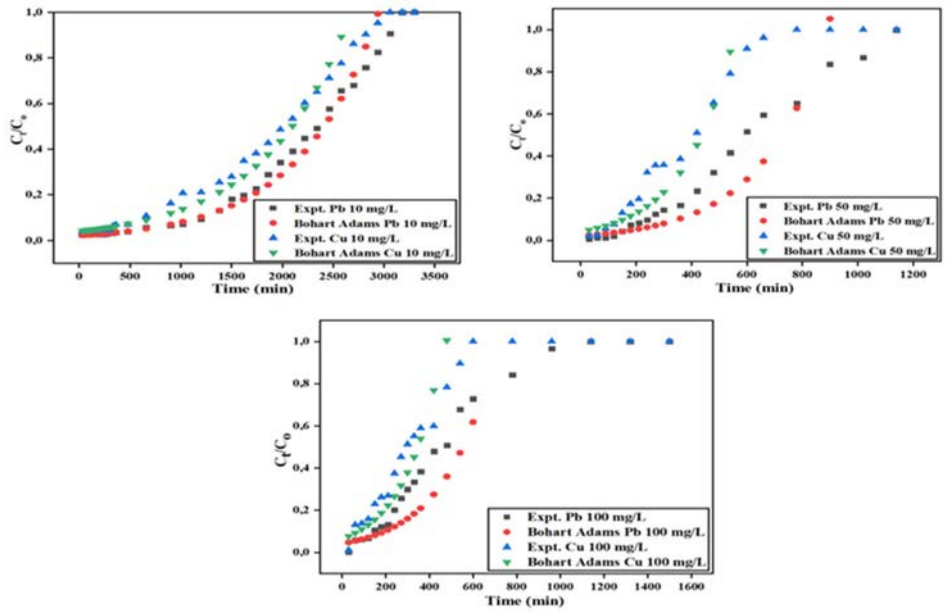

Figure 8: Breakthrough curves of Pb^{2+} and Cu^{2+} at initial concentration of 10, 50 and 100 mg/L fitted into Bohart–Adams model.

Table 2: Breakthrough model data for binary biosorption of Cu^{2+} and Pb^{2+}.

Parameter	Thomas			Yoon–Nelson			Bohart–Adams		
	K_{Th} *10^{-4} ($Lmin^{-1}$ mg^{-1})	q_o (mg/g)	R^2	K_{YN} (min^{-1})	τ (min)	R^2	K_{BA}*10^{-4} ($Lmin^{-1}$ mg^{-1})	No (mg/L)	R^2
Metal ion concentration (10mg/L)									
Pb	2.10	10.09	0.96	0.01	2018.38	0.95	1.30	7089.11	0.91
Cu	2.40	9.07	0.98	0.01	1814.53	0.98	1.70	6438.03	0.97
Metal ion concentration (50mg/L)									
Pb	1.54	14.78	0.93	0.01	591.26	0.92	0.86	10690.64	0.81
Cu	2.00	9.34	0.97	0.01	373.50	0.96	1.14	6731.49	0.84
Metal ion concentration (100mg/L)									
Pb	0.77	23.56	0.86	0.01	471.12	0.86	0.45	17012.46	0.61
Cu	0.95	15.95	0.88	0.01	319.00	0.87	0.59	11182.03	0.69

this tendency was seen when the starting concentration increased. While the values of q_o for Pb^{2+} are higher than Cu^{2+} in all the various initial concentrations, the values of K_{Th} for Pb^{2+} are lower than Cu^{2+} under all conditions. The initial concentration correlation coefficients (R^2) fall between 0.861 to 0.979, indicating a good fit between the experimental data and the Thomas model.

3.3.2 Yoon–Nelson model

The Yoon–Nelson model graphs shown in Fig. 7 illustrated that while the time it takes for the effluent concentration to reach 50% of the initial concentration (τ) decreased as the initial concentration increased, the Yoon–Nelson coefficient K_{YN} increased. Furthermore, the correlation coefficient (R^2) was similar to the Thomas model, ranging from 0.86 to 0.977.

3.3.3 Bohart–Adams model

The maximum volumetric sorption capacity (N_o) increased as the initial concentration increased, whereas the Bohart–Adams constant (K_{BA}) decreased, according to the Bohart–Adams model displayed in Fig. 8. This suggests that the adsorption efficiency of the metal ions increased with an increase in the initial metal ion concentration. The model shows that the adsorption uptake of Pb^{2+} was higher than Cu^{2+} in the concentrations considered. The correlation coefficient (R^2) ranged from 0.606 to 0.966 which differs from the Thomas and Yoon–Nelson models. The difference in the R^2 can be attributed to the different symmetry and shape of the Pb^{2+} and Cu^{2+} breakthrough curves obtained from fitting the experimental data with the Bohart–Adams model compared with those obtained from the Thomas and Yoon–Nelson models. Hence, the experimental data agree well with the Thomas and Yoon–Nelson models at the initial concentrations considered. The Bohart–Adams model's simplicity and underlying assumptions that intraparticle diffusion and external mass transfer barriers are negligible and that biosorption kinetics is dictated by the surface chemical interaction between the biosorbent and the adsorbate also make it noteworthy. The Bohart–Adams model yielded lower R^2 values, indicating that the experimental data may not adequately match the model. However, the model parameters provided valuable information regarding the metal ion adsorption uptake.

4 CONCLUSION

In this study, orange peels were found to be an effective bio-waste for the continuous removal of both Cu^{2+} and Pb^{2+} from an aqueous solution, in a fixed-bed column. The results showed that the breakthrough curves for the removal of Pb^{2+} and Cu^{2+} are dependent on the initial metal ion concentration. The S-shaped breakthrough curves of Pb^{2+} and Cu^{2+} binary systems are typical of breakthrough curves for adsorption. Since the binding site was rapidly saturated, a rise in the influent metal ion concentration produced a steeper breakthrough curve that moved the curve closer to the origin. For both metals, the breakthrough time dropped as the starting concentration increased. Because the Cu^{2+} breakthrough curves reached a breakthrough point more quickly than Pb^{2+}, it is possible that Cu^{2+} has less affinity for the binding sites on the biosorbent surface. Pb^{2+} binding strength affected its adsorption capacity, which was consistently greater than Cu^{2+} for all concentrations. When considering the experimental data for initial concentrations, the Yoon–Nelson and Thomas models performed better than the Bohart–Adams model. In order to advance from laboratory-scale of Pb^{2+} and Cu^{2+} biosorption process technology to pilot-scale and ultimately industrial-scale levels, more mathematically model studies regarding Pb^{2+} and Cu^{2+} desorption and orange peels regeneration resulting from multiple consecutive biosorption–desorption cycles are required.

ACKNOWLEDGEMENTS

The authors wish to appreciate the National Research Foundation (NRF) South Africa for their financial assistance, Durban University of Technology (DUT), Mangosuthu University of Technology (MUT) and University of KwaZulu-Natal (UKZN) Pietermaritzburg Campus for the privilege to use some of the equipment in their laboratories for the analytical work conducted in this study.

REFERENCES

[1] Liu, J. et al., Water scarcity assessments in the past, present, and future. *Earth's Future*, **5**(6), pp. 545–559, 2017.

[2] Volesky, B., Removal and recovery of heavy metals by biosorption. *Biosorption of Heavy Metals*, pp. 7–43, 1990.

[3] Singh N.B. et al., Water purification by using Adsorbents: A review. *Environmental Technology and Innovation*, **11**, pp. 187–240, 2018.

[4] Raouf, M.S. & Raheim, A.R.M., Removal of heavy metals from industrial waste water by biomass-based materials: A review. *Journal of Pollution Effects and Control*, **05**(01), 2016.

[5] Orts, F. et al., Study of the reuse of industrial wastewater after electrochemical treatment of textile effluents without external addition of chloride. *International Journal of Electrochemical Science*, pp. 1733–1750, 2019.

[6] Obotey Ezugbe, E. & Rathilal S., Membrane technologies in wastewater treatment: A review. *Membranes (Basel)*, **10**(5), 2020.

[7] Tee, G.T., Gok, X.Y & Yong W.F., Adsorption of pollutants in wastewater via biosorbents, nanoparticles and magnetic biosorbents: A review. *Environmental Research*, **212**(Pt B), 113248, 2022.

[8] Chakraborty, R. et al., Adsorption of heavy metal ions by various low-cost adsorbents: A review. *International Journal of Environmental Analytical Chemistry*, **102**(2), pp. 342–379, 2020.

[9] Syeda, H.I. et al., Biosorption of heavy metals from aqueous solution by various chemically modified agricultural wastes: A review. *Journal of Water Process Engineering*, **46**, 2022.

[10] Gryko, K., Kalinowska, M. & Świderski, G., The use of apple pomace in removing heavy metals from water and sewage. *Innovations-Sustainability-Modernity-Openness Conference (ISMO'21)*, 2021.
[11] Harripersadth, C., Evaluating the performance of an eggshell-bagasse biosorption system in removing lead and cadmium from aqueous solutions. *Chemical Engineering*, Durban University of Technology, pp. 1–109, 2021.
[12] Mondal, N.K. & Roy A., Potentiality of a fruit peel (banana peel) toward abatement of fluoride from synthetic and underground water samples collected from fluoride affected villages of Birbhum district. *Applied Water Science*, **8**(3), 2018.
[13] Afolabi, F.O., Musonge, P. & Bakare, B.F., Bio-sorption of a bi-solute system of copper and lead ions onto banana peels: characterization and optimization. *Journal of Environmental Health Science and Engineering*, 2021.
[14] Ahmad, H., Ee, C.J. & Baharudin, N.s., A preliminary study for removal of heavy metals from acidic synthetic wastewater by using pressmud-rice husk mixtures. *IOP Conference Series: Earth and Environmental Science*, **36**, pp. 1–8, 2016.
[15] Semerjian, L., Removal of heavy metals (Cu, Pb) from aqueous solutions using pine (Pinus halepensis) sawdust: Equilibrium, kinetic, and thermodynamic studies. *Journal of Environmental Technology Innovation*, **12**, pp. 91–103, 2018.
[16] Vera, L.M. et al., Fixed bed column modeling of lead (II) and cadmium (II) ions biosorption on sugarcane bagasse. *Journal of Environmental Engineering Research*, **24**(1), pp. 31–37, 2018.
[17] Qin, H. et al., The improved methods of heavy metals removal by biosorbents: A review. *Environmental Pollution*, **258**, 113777, 2020.
[18] Akpomie, K.G. & Conradie, J., Banana peel as a biosorbent for the decontamination of water pollutants. A review. *Environmental Chemistry Letter*, **18**, pp. 1085–1112, 2020.
[19] Afolabi, F.O., Musonge, P. & Bakare, B.F., Adsorption of copper and lead ions in a binary system onto orange peels: Optimization, equilibrium, and kinetic study. *Sustainability*, **14**(17), 2022.
[20] Arim, A.L. et al., Experimental and mathematical modelling of Cr(III) sorption in fixed-bed column using modified pine bark. *Journal of Cleaner Production*, **183**, pp. 272–281, 2018.
[21] Taka, A.L. et al., Chitosan nanocomposites for water treatment by fixed-bed continuous flow column adsorption: A review. *Carbohydrate Polymers*, 117398, 2020.
[22] Carneiro, M.A. et al., Current trends of arsenic adsorption in continuous mode: Literature review and future perspectives. *Sustainability*, **13**(3), p. 1186, 2021.
[23] Oliveira, R.F. et al., Cr (VI) adsorption in batch and continuous scale: A mathematical and experimental approach for operational parameters prediction. *Environmental Technology and Innovation*, **20**, 101092, 2020.
[24] Martín-Lara, M.A. et al., Binary biosorption of copper and lead onto pine cone shell in batch reactors and in fixed bed columns. *International Journal of Mineral Processing*, **148**, pp. 72–82, 2016.